

A New Analysis of Variance Reduced Stochastic Proximal Methods for Composite Optimization with Serial and Asynchronous Realizations

Yue Yu and Longbo Huang

Institute for Interdisciplinary Information Sciences, Tsinghua University
 yu-y14@mails.tsinghua.edu.cn, longbohuang@tsinghua.edu.cn

Abstract

We provide a comprehensive analysis of stochastic variance reduced gradient (SVRG) based proximal algorithms, both with and without momentum, in serial and asynchronous realizations. Specifically, we propose the Prox-SVRG⁺⁺ algorithm, and prove that it has a linear convergence rate with a small epoch length and we obtain an $O(1/\epsilon)$ complexity in non-strongly convex case. Then, we propose a momentum accelerated algorithm, called Prox-MSVRG⁺⁺, and show that it achieves a complexity of $O(1/\sqrt{\epsilon})$. After that, we develop two asynchronous versions based on the above serial algorithms and provide a general analysis under nonconvex and non-strongly convex cases respectively. Our theoretical results indicate that the algorithms can achieve a potentially significant speedup when implemented with multiple servers. We conduct extensive experiments based on 4 real-world datasets on an experiment platform with 11 physical machines. The experiments validate our theoretical findings and demonstrate the effectiveness of our algorithms.

1 Introduction

In this paper, we study the following finite-sum composite minimization problem

$$\min_{x \in \Omega} F(x) = f(x) + h(x), \quad f(x) = \frac{1}{n} \sum_{i=1}^n f_i(x), \quad (1)$$

where $f(x)$ has L -Lipschitz continuous gradient and $h(x)$ is convex but possibly nonsmooth. The domain $\Omega \subseteq \mathbb{R}^d$ is a convex set. This formulation arises in many machine learning, operations research, and statistics problems [16, 12, 2], e.g., classification or regression. In these problems, n often denotes the data size (number of samples), and $f_i(x)$ denotes the loss function for sample i , and $h(x)$ represents certain regularizer.

To tackle the nonsmooth nature of function $h(x)$, one common method is to use the proximal operator [28, 38], which is formed as $\text{prox}_{\eta h}(x) = \arg \min_y [h(y) - \frac{1}{2\eta} \|y - x\|^2]$. This proximal operator has different meanings with different $h(x)$ functions, e.g., when $h(x)$ is the indicator function of a closed convex set, the proximal operator becomes a projection.

Many first-order stochastic algorithms have been proposed for solving (1). In this paper, we focus on two popular schemes, namely, the stochastic variance reduced gradient (SVRG) scheme [12, 45] and the momentum acceleration scheme [29, 30]. These two schemes have shown great promise in practice and received much attention.

Along the line of variance reduction, many algorithms have been proposed, including SAG [39], SAGA [7], MISO [24], SVRG [12, 45], etc. By reducing the variance of stochastic gradient, these algorithms significantly accelerate algorithm convergence, e.g., converging linearly for the strongly convex problem while stochastic gradient descent (SGD) only has a rate of $O(1/\epsilon)$, where ϵ is the proximity to the optimal value. Among these algorithms, SVRG [12, 43] receives much consideration because of its low memory cost. Although it was originally designed for strongly convex objectives, its (and its variants') convergence property for non-strongly convex problems, i.e., general convex, has also been studied recently, e.g., [4, 17, 35]. However, existing results cannot explain some common implementations in practice. For instance, the epoch length is empirically set to be much smaller than the theoretical optimal value condition number (or n) for achieving a good performance. In this paper, we establish a novel argument inspired by momentum technique analysis and obtain new theoretical findings for SVRG based proximal methods.

The momentum acceleration technique originated by Nesterov, e.g., [29, 30], on the other hand, has also been shown to achieve speedup over first-order algorithms, e.g., gradient descent (GD). Recent works including [2, 10] further combine SVRG with momentum, and achieve a gradient complexity of $O(1/\sqrt{\epsilon})$, by introducing two auxiliary momentum variables. We propose a new accelerated version of SVRG with one momentum variable, called Prox-MSVRG⁺⁺, to achieve the $O(1/\sqrt{\epsilon})$ complexity. Reducing the number of momentum variables from two to one is nontrivial. It makes our algorithm more concise and provides a new way to utilize momentum.

To make our algorithms suitable for implementation in large-scale systems, we further propose two asynchronous versions of SVRG based proximal methods (asynchronous Prox-SVRG and asynchronous Prox-MSVRG⁺⁺). Existing works on SVRG based asynchronous algorithms often assume strong convexity [27, 36, 46] or do not consider a nonsmooth composite structure [26, 36, 46, 48, 11]. Therefore, the performance under more general conditions is still missing. Our results fill this gap and are established without requiring such assumptions.

Contributions. In this paper, we make the following main contributions.

- We provide a new analysis for stochastic variance reduced proximal methods based on a novel algorithm Prox-SVRG⁺⁺. Specifically, we first prove that SVRG based algorithms can achieve a linear convergence rate with a much shorter epoch length for strongly convex objectives. Then, in the non-strongly convex case, we remove the dependence of ϵ in the coefficient of n when the domain of (1) is bounded.
- Based on the analysis of Prox-SVRG⁺⁺, we propose a momentum accelerated algorithm, Prox-MSVRG⁺⁺, and show that it achieves a gradient complexity of $O((n + \sqrt{nL})/\sqrt{\epsilon})$. Compared to results in [2, 10], our algorithm has a simpler form and makes use of a single auxiliary momentum variable. This provides an alternative way for achieving acceleration.
- We prove that the asynchronous implementation of Prox-SVRG [43, 37] achieves a complexity of $O(n + Ln^{2/3}/\epsilon)$ for nonconvex objectives and achieves a linear speedup. We establish our results without requiring two common assumptions in the asynchronous literature, i.e., strong convexity and sparsity, e.g., [27, 46].
- We further study asynchronous Prox-MSVRG⁺⁺, and show that it achieves a gradient complexity of $\tilde{O}(1/\sqrt{\epsilon})$. To the best of our knowledge, this is the first momentum acceleration result without the strong convexity assumption in the asynchronous setting. Moreover, our results confirm that momentum based algorithms prefer a high gradient accuracy for achieving acceleration, a result also observed in previous works [2, 13].
- We conduct experiments with 4 real-world datasets on a 11-server testbed, to validate our theoretical results. The results demonstrate that our schemes outperform existing algorithms.

2 Other Related Work

(SVRG based schemes) [4] proposed SVRG⁺⁺ and proved the current best known gradient complexity of $O(n \log \frac{1}{\epsilon} + \frac{L}{\epsilon})$ for convex objectives in SVRG family. [35, 3, 37] focused on nonconvex objective functions and proved an $\tilde{O}(1/\epsilon)$ complexity, among which [37] considered an objective with regularizer function $h(x)$. Many works also combined Nesterov or momentum acceleration technique to SVRG to achieve the optimal rate $O(1/\sqrt{\epsilon})$ [2, 10, 32, 21]. [40] proposed a similar SVRG-based algorithm, though with a different epoch length setting. We provide different theoretical results based on our new analysis. [41] provided an acceleration scheme with one auxiliary variable, but only provided proofs for smooth objectives.

(Asynchronous schemes) Designing asynchronous algorithms has been another area of active research. Asynchronous versions of SGD and stochastic proximal gradient have been investigated both in theory and practice, though only achieving a slower $O(1/\epsilon^2)$ rate [34, 1, 47, 19, 20, 23]. Asynchronous variance reduction based algorithms are also proposed to accelerate convergence. Besides the work mentioned in Section 1, many other work, e.g., [25, 15], analyze the lock-free asynchronous implementations assuming strongly convex objectives. [9] provides a new analysis of asynchronous Proximal SVRG with a block separable $h(x)$.

Our work distinguishes itself from the above results as follows. (i) We conduct a comprehensive analysis for SVRG based proximal algorithms, and consider both serial and asynchronous implementations. (ii) We relax the strong convexity and sparsity assumptions commonly assumed for asynchronous algorithms. This makes our results more general and have a larger scope of applications.

3 Preliminary

In this paper, we adopt *gradient complexity* for measuring the efficiency of first-order algorithms, which equals to the total number of gradient calculations for obtaining an ϵ -error point x .¹ This metric has been commonly adopted in the literature, sometimes under different names, e.g., [4, 17, 35].

Stochastic Variance Reduced Gradient (SVRG): SVRG is designed for retaining the efficiency of SGD and the fast rate of GD. It carries out the update process in epochs, each containing m inner iterations. At the beginning of each epoch s , it records a snapshot \tilde{x}^{s-1} and computes its full gradient $\tilde{\mu}$. Then, in each inner iteration, it forms the following (variance reduced) stochastic gradient:

$$\tilde{\nabla} f_{i_k^s}(x_{k-1}^s) = \nabla f_{i_k^s}(x_{k-1}^s) - \nabla f_{i_k^s}(\tilde{x}^{s-1}) + \tilde{\mu}. \quad (2)$$

Existing results show that SVRG attains a linear rate if the epoch length is greater than the condition number of the objective. The key reasons for this acceleration lie in the facts that $\tilde{\nabla} f_{i_k^s}(x_k^s)$ is unbiased, and that the variance $\mathbf{E}\|\tilde{\nabla} f_{i_k^s}(x_k^s) - \nabla f(x_k^s)\|^2$ decreases to zero as $x_k^s \rightarrow x^*$ [12, 43].

Notation. We denote x^* as an optimal solution of (1). For x_k^s , the superscript s indicates the s -th epoch, the subscript k denotes the k -th inner iteration. For a set I_k^s , $|I_k^s|$ denotes its size. Denote $\Delta \triangleq F(\tilde{x}^0) - F(x^*)$, $\Gamma \triangleq \|\tilde{x}^0 - x^*\|^2$, where \tilde{x}^0 is the start point of our algorithms. $\nabla f_i(x)$ is the stochastic gradient calculated on a sample i . d is the dimension of x . n equals to the number of samples. We also define $\rho(b) \triangleq \frac{n-b}{b(n-1)}$ for short, where b is a positive constant. $\|\cdot\|$ represents for L_2 -norm if without special annotation. The notation $\tilde{O}(f)$ denotes $O(f \cdot \text{polylog}(f))$.

Assumptions. We state the assumptions made in this paper. These assumptions are mild and are often assumed in the literature, e.g., [12, 4, 17, 44].

Assumption 1. Each $f_i(x)$ has L -Lipschitz continuous gradient ($L > 0$) in the domain Ω , i.e.,

$$\|\nabla f_i(x) - \nabla f_i(y)\| \leq L\|x - y\|, \quad \forall x, y \in \Omega. \quad (3)$$

Assumption 2. Function $F(x)$ is μ -strongly convex, such that for any $x \in \Omega$:

$$F(x) \geq F(x^*) + (\mu/2)\|x - x^*\|^2, \quad \mu > 0. \quad (4)$$

Assumption 3. The stochastic gradient is unbiased, i.e., for the sampled mini-batch I_k^s with size b ,

$$\mathbf{E}_{I_k^s} \left[\sum_{i \in I_k^s} \nabla f_i(x) \right] = b \nabla f(x). \quad (5)$$

Moreover, the random variables sampled in different iterations are independent.

4 A New Proximal Gradient with SVRG

In this section, we propose a new algorithm Prox-SVRG⁺⁺ to solve (1). The algorithm is shown in Algorithm 1. It adopts a mini-batch scheme to both reduce the variance of stochastic gradient and accelerate convergence. The main difference between Algorithm 1 and other SVRG based proximal algorithms, e.g., [43, 4], is the use of auxiliary variable y_k^s and parameters η_s and θ_s . Choosing right values for η_s and θ_s is the key to obtain a tighter bound. It can also be verified that Algorithm 1 and SVRG in [12] are equivalent if $h(x) = 0$ and the step-size used by SVRG [12] equals to $\eta_s \theta_s$.

4.1 Analysis

We state the performance of Prox-SVRG⁺⁺ in the following theorem. Recall that $\rho(b) \triangleq \frac{n-b}{b(n-1)}$.

Theorem 1. Suppose $f(x)$ is convex and Assumptions 1, 3 hold. Let $\eta_s = \frac{1}{2L\theta_s}$. If for all $s \geq 1$ and $b = |I_k^s|$, we have $\theta_s + \rho(b) \leq 1$, then under Algorithm 1,

$$\mathbf{E}[F(\tilde{x}^s) - F(x^*)] \leq \mathbf{E}[(1 - \theta_s)(F(\tilde{x}^{s-1}) - F(x^*)) + L\theta_s^2/m * (\|y_0^s - x^*\|^2 - \|y_m^s - x^*\|^2)].$$

¹For an accuracy measurement $M(x)$, an ϵ -error point x satisfies $M(x) \leq \epsilon$. For example, $M(x)$ can be chosen as $M(x) = F(x) - F(x^*)$ for a convex problem, where x^* is an optimal solution.

Algorithm 1 Prox-SVRG⁺⁺

```
1: Input:  $S, m, b, \tilde{x}^0, \theta_0, \eta_0$ ;  
2: for  $s = 1, 2, \dots, S$  do  
3:   update  $\theta_s$  and  $\eta_s$ ;  
4:    $x_0^s = y_0^s = \tilde{x}^{s-1}$ ;  
5:    $\tilde{\mu} = \frac{1}{n} \sum_{i=1}^n \nabla f_i(\tilde{x}^{s-1})$ ;  
6:   for  $k = 1$  to  $m$  do  
7:     uniformly and independently sample a mini-batch  $I_k^s$  with size  $b$  from  $\{1, \dots, n\}$ ;  
8:      $\tilde{\nabla} f_{I_k^s}(x_{k-1}^s) = \frac{1}{|I_k^s|} \sum_{i_k^s \in I_k^s} \left( \nabla f_{i_k^s}(x_{k-1}^s) - \nabla f_{i_k^s}(\tilde{x}^{s-1}) \right) + \tilde{\mu}$ ;  
9:      $y_k^s = \text{prox}_{\eta_s h}(y_{k-1}^s - \eta_s \tilde{\nabla} f_{I_k^s}(x_{k-1}^s))$ ;  
10:     $x_k^s = \tilde{x}^{s-1} + \theta_s (y_k^s - \tilde{x}^{s-1})$ ;  
11:   end for  
12:    $\tilde{x}^s = \frac{1}{m} \sum_{k=1}^m x_k^s$ ;  
13: end for  
14: Output:  $\tilde{x}^S$ .
```

Denote $\kappa \triangleq L/\mu$, the condition number of $F(x)$. We have the following immediate corollary, which covers the theoretical findings of [12].

Corollary 1. *Under conditions in Theorem 1,*

(a) *if Assumption 2 holds. Let $\theta_s \equiv \theta$, $\eta_s \equiv \eta$ and $\eta * \theta = \frac{1}{2L}$, then under Algorithm 1,*

$$\mathbf{E}[F(\tilde{x}^s) - F(x^*)] \leq (1 - \theta + 2\kappa\theta^2/m) \mathbf{E}[F(\tilde{x}^{s-1}) - F(x^*)].$$

(a.1) *If $m = 2\kappa$ and $\theta = \frac{1}{2}$, define $\alpha \triangleq (1 - \theta + 2\kappa\theta^2/m) = \frac{3}{4}$. The gradient complexity of Algorithm 1 equals to $O((n + \kappa) \log \frac{1}{\epsilon})$.*

(a.2) *If $m = 2\kappa^\beta$ and $\theta = \frac{1}{2\kappa^{1-\beta}}$, where $\beta \in (0, 1)$, the gradient complexity of Algorithm 1 is $O\left((n + \kappa^\beta) \frac{1}{\Lambda} \log \frac{1}{\epsilon}\right)$, where $\Lambda = \log \frac{4\kappa^{1-\beta}}{4\kappa^{1-\beta} - 1}$.*

(b) *if $f(x)$ is non-strongly convex and the domain Ω of x is bounded by a constant D , such that $\forall x, y \in D, \|x - y\|^2 \leq D$. Let $\theta_s = \frac{2}{s+2}$, $\eta_s = \frac{1}{2L\theta_s}$, then*

$$\mathbf{E}[F(\tilde{x}^S) - F(x^*)] \leq 4\Delta/S^2 + 4LD/(mS).$$

Setting $m = n$, the asymptotic gradient complexity of Algorithm 1 equals to $O(n + LD/\epsilon)$.

Remarks. There usually exists a tradeoff between the epoch length m and the theoretical gradient complexity, especially when κ is large (κ is often approximated by n in practice). Note that the results in Corollary 1 (a) present linear rate convergence in two parameter settings and show that, if m is enlarged to 2κ from $2\kappa^\beta$, the gradient complexity becomes smaller. However, if m is large, x_{k-1}^s may move far away from \tilde{x}^{s-1} , which introduces a large variance in $\tilde{\nabla} f_{I_k^s}(x_{k-1}^s)$ and slows down convergence in practice [4]. Therefore, m is often empirically chosen to be smaller than κ when it is large. However, existing theoretical results only show that SVRG attains a linear rate when $m \geq \kappa$ [43, 12]. Our new results in Corollary 1(a.2) provide a reasonable explanation that why a much smaller m can also achieve a linear rate.

Corollary 1 (b) shows that we obtain a complexity of $O(n + LD/\epsilon)$ in the non-strongly convex case with a bounded region. The possibility of the algorithm going outside the domain is avoided by the proximal operator in Step 9 (similarly for Theorem 4, see the Supplementary Material for details). Compared to the best known result $O(n \log \frac{1}{\epsilon} + \frac{LD}{\epsilon})$ of SVRG⁺⁺ [4], we remove the factor $\log(1/\epsilon)$ from the first term containing n . Moreover, we show in Section 5 that the procedures of Prox-SVRG⁺⁺ can be easily extended to contain momentum acceleration.

5 Momentum Acceleration of Prox-SVRG⁺⁺

Steps 9-10 in Algorithm 1 are common steps in momentum or Nesterov-based algorithms [2, 33, 21]. The update of x_k^s combines history information \tilde{x}^{s-1} and the latest auxiliary variable y_k^s . However, this ‘‘momentum’’ information is

Algorithm 2 Momentum Accelerated Prox-SVRG⁺⁺ (Prox-MSVRG⁺⁺)

- 1: Input: $S, m, b, \tilde{x}^0, y_m^0 = \tilde{x}^0$;
 - 2: **for** $s = 1, 2, \dots, S$ **do**
 - 3: $\theta_s = 2/(s + 2), \eta_s = 1/(2L\theta_s)$;
 - 4: $x_0^s = \theta_s y_m^{s-1} + (1 - \theta_s)\tilde{x}^{s-1}, y_0^s = y_m^{s-1}$;
 - 5: perform the same procedures as Steps 5 – 12 in Algorithm 1;
 - 6: **end for**
 - 7: Output: \tilde{x}^S .
-

lost at the beginning of each epoch, since y abandons its accumulated step and is restored to \tilde{x}^{s-1} . Thus, Algorithm 1 does not possess momentum acceleration.

In this section, we show that the momentum step in Algorithm 1 can make a difference if we slightly change the initialization of x, y at the beginning of each epoch. Specifically, in Algorithm 2, y_0^s inherits its value of the last epoch and x_0^s is updated using the accumulated momentum (Step 4). The other steps remain unchanged as in Algorithm 1. We show in the following theorem that these two simple (but critical) changes bring a significant acceleration.

Theorem 2. *Suppose $f(x)$ is convex and Assumptions 1, 3 hold. Then, with $|I_k^s| = b$, if for all $s \geq 1$, $\rho(b) < 1/3$, Algorithm 2 achieves (recall $\Delta \triangleq F(\tilde{x}^0) - F(x^*), \Gamma \triangleq \|\tilde{x}^0 - x^*\|^2$)*

$$\mathbf{E}[F(\tilde{x}^S) - F(x^*)] \leq 4\Delta/S^2 + 4L\Gamma/(mS^2). \quad (6)$$

Corollary 2. *Let $m = n$. The gradient complexity of Algorithm 2 is $O((n + \sqrt{nL})/\sqrt{\epsilon})$.*

The above result shows that the acceleration from $O(1/\epsilon)$ to $O(1/\sqrt{\epsilon})$ can be achieved with just one auxiliary variable, Table 1 in the Supplementary Material summarizes the gradient complexities and numbers of auxiliary variables of several closely related acceleration algorithms.

Till now, we have provided analysis of Prox-SVRG⁺⁺ and Prox-MSVRG⁺⁺, both being serial (centralized) algorithms. In the following sections, we focus on analyzing the convergence property of asynchronous Prox-SVRG and asynchronous Prox-MSVRG⁺⁺.

6 Asynchronous Proximal SVRG

Asynchronous algorithms are widely used in large-scale machine learning and optimization problems [20, 23], where tasks are often jointly solved by multiple servers (threads in multi-core system). In this section, we investigate the asynchronous Prox-SVRG algorithm studied in the literature before, e.g., [27], and focus on the *consistent read setting*, i.e., during execution, the algorithm guarantees the atomic operation on the whole vector of x . As a result, the value of x each worker reads always equals to certain x values after a complete update. Such asynchronous implementations have been adopted in parameter servers [18] and asynchronous distributed neural networks [6].

However, the analysis of asynchronous Prox-SVRG often assumes strong convexity or sparsity of the objective. Below we provide a new analysis under more general conditions.

6.1 Algorithm

We start with the implementation setting and describe the algorithm. Consider a system consisting of one master and multiple workers, e.g., parameter-servers. The master maintains the latest updated variable x and a clock. Each worker ω has access to the full datasets and keeps a disjoint partition D_ω of data with size n_ω . All workers work independently and communicate with the master to access x .

As shown in Algorithm 3, at the beginning of each epoch, the master broadcasts a snapshot variable \tilde{x}^{s-1} . Then, each worker calculates the gradient $\nabla f_\omega(\tilde{x}^{s-1})$ and sends it to the master. After that, the master machine combines these information to compute the full gradient $\tilde{\mu}$. Then, in the inner iteration, each worker uniformly and independently samples a mini-batch I_t^s with size b , to form the stochastic gradients shown in Step (w_3). After that, it sends them to the master.

Upon receiving the gradients, the master combines them with the full gradient $\tilde{\mu}$ to calculate the stochastic variance reduced gradient (Steps m_3 and m_4), without requiring them to be synchronized. Here, in order to ensure the atomic

Algorithm 3 Asynchronous Prox-SVRG

Input: $S, m, b, \tilde{x}^0 = x_m^0, \eta;$ **for** $s = 1, 2, \dots, S$ **do**

For master:

 (m_1) broadcast \tilde{x}^{s-1} and update $x_0^s = x_m^{s-1};$ (m_2) aggregate gradients from all workers and compute $\tilde{\mu} = \sum_{\omega} \frac{n_{\omega}}{n} \nabla f_{\omega}(\tilde{x}^{s-1});$

For each worker:

 (w_1) calculate $\nabla f_{\omega}(\tilde{x}^{s-1}) = \frac{1}{n_{\omega}} \sum_{i \in D_{\omega}} \nabla f_i(\tilde{x}^{s-1})$ and send it to master; **for** $t = 0$ to $m - 1$ **do**

For master:

 (m_3) receive $\frac{1}{|I_t^s|} \sum_{i_t^s \in I_t^s} \nabla f_{i_t^s}(x_{D(t)}^s), \frac{1}{|I_t^s|} \sum_{i_t^s \in I_t^s} \nabla f_{i_t^s}(\tilde{x}^{s-1})$ from a specific worker; (m_4) compute $u_t^s = \frac{1}{|I_t^s|} \sum_{i_t^s \in I_t^s} \left(\nabla f_{i_t^s}(x_{D(t)}^s) - \nabla f_{i_t^s}(\tilde{x}^{s-1}) \right) + \tilde{\mu};$ (m_5) $x_{t+1}^s = \text{prox}_{\eta h}(x_t^s - \eta u_t^s);$

For each worker:

 (w_2) retrieve $x_{D(t)}^s$ from master and sample a mini-batch I_t^s from $\{1, \dots, n\};$ (w_3) compute $\frac{1}{|I_t^s|} \sum_{i_t^s \in I_t^s} \nabla f_{i_t^s}(x_{D(t)}^s), \frac{1}{|I_t^s|} \sum_{i_t^s \in I_t^s} \nabla f_{i_t^s}(\tilde{x}^{s-1})$ and send to master; **end for** $\tilde{x}^s = x_m^s;$ **end for**Output: Randomly and uniformly choose from $\{\{x_t^s\}_{t=0}^{m-1}\}_{s=1}^S.$

operation of x , we assume that when the x value being updated, workers cannot read its value. This “consistent read” condition can be efficiently guaranteed in computer network and is commonly assumed in the literature [20, 11].

Since the workers asynchronously pull and push data during inner iterations, at time t , the master may use delayed gradients calculated based on a previous state $x_{D(t)}^s$, where $D(t) \leq t$. While this can cause the “stale” gradient problem, we show in Theorem 3 that the negative influence of delayed gradient vanishes asymptotically, provided that the gradient delay is reasonably moderate. Also note that there is a synchronization at the beginning of each epoch. This is a typical requirement of the SVRG method [36], and does not impact performance since we only perform it once per epoch.

6.2 Convergence Analysis

We first state an additional assumption needed for the gradient delay. This assumption can often be satisfied in practical computing systems and is commonly assumed in the literature, e.g., [20, 23, 36].

Assumption 4. *The maximum gradient delay is upper bounded for all time by some finite constant $\tau > 0$, i.e., $t - D(t) \leq \tau, \forall t$.*

In this section, we remove the convex condition of $f(x)$, making our results cover more applications in practice. In this case, instead of $F(x) - F(x^*)$, we apply the *gradient mapping* term $G_{\eta}(x) = \frac{1}{\eta}[x - \text{prox}_{\eta h}(x - \eta \nabla f(x))]$ to measure the convergence property. This metric is commonly used in analyzing nonconvex proximal algorithms, such as [37, 42, 8]. It can be verified that $\|G_{\eta}(x)\| = 0$ when x is a stationary point. Thus, an ϵ -error point x implies $\|G_{\eta}(x)\|^2 \leq \epsilon$.

Theorem 3. *If $f(x)$ is nonconvex and Assumptions 1, 3, and 4 hold. Let $m = \lceil n^{\frac{1}{3}} \rceil$, $b = \lceil 8n^{\frac{2}{3}} \rceil$ and $\eta = \frac{\sigma}{L}$ where $0 < \sigma < \frac{1}{3}$. If delay $\tau \leq \sqrt{\frac{1-\sigma-\sigma^2}{2\sigma^2}}$, denote x_{out} as the output of Algorithm 3, then*

$$\mathbf{E}\|G_{\eta}(x_{out})\|^2 \leq 2L\Delta/[T\sigma(1-2\sigma)].$$

Moreover, the gradient complexity is $O(n + Ln^{\frac{2}{3}}/\epsilon)$.

Algorithm 4 Asynchronous Prox-MSVRG⁺⁺ (Master Node)

Input: $S, m, b, \tilde{x}^0, y_m^0 = \tilde{x}^0$;
for $s = 1, 2, \dots, S$ **do**
 update θ_s, η_s and broadcast \tilde{x}^{s-1} ;
 $x_0^s = \theta_s y_0^s + (1 - \theta_s) \tilde{x}^{s-1}, y_0^s = y_m^{s-1}$;
 aggregate gradients from all workers and compute $\tilde{\mu} = \sum_{\omega} \frac{n_{\omega}}{n} \nabla f_{\omega}(\tilde{x}^{s-1})$;
 for $t = 0$ to $m - 1$ **do**
 perform the same procedures as Step (m₃) and (m₄) in Algorithm 3;
 $y_{t+1}^s = \text{prox}_{\eta_s h}(y_t^s - \eta_s u_t^s)$;
 $x_{t+1}^s = \tilde{x}^{s-1} + \theta_s (y_{t+1}^s - \tilde{x}^{s-1})$;
 end for
 $\tilde{x}^s = \frac{1}{m} \sum_{t=0}^{m-1} x_{t+1}^s$;
end for
Output: \tilde{x}^S .

Remarks. The above gradient complexity is the same as that of serial Prox-SVRG [37]. Thus, a linear speedup can be attained, because workers take actions in parallel. Note that using gradient complexity to measure speedup is a common practice in the literature, e.g., [20, 27, 11]. To better demonstrate the efficiency of our algorithms, we also provide the running time speedups in experiments. In addition, we relax the strong convexity and sparsity assumptions in related work on asynchronous Prox-SVRG [27]. Recent work [11] proved an $O(n + Ln/\epsilon)$ complexity for obtaining a stationary point with the step size $O(\frac{1}{Ln^\alpha})$ for asynchronous SVRG. We focus on a more general nonsmooth composite problem and the above result shows that we can use a step size that is independent of n , and achieve a lower gradient complexity.

7 Momentum Accelerated Asynchronous Prox-MSVRG⁺⁺

In the analysis of serial algorithms, we have established the acceleration of momentum to Prox-SVRG⁺⁺. In this section, we show that momentum also applies in asynchronous implementations. The procedures of the master node is summarized in Algorithm 4, and the steps for workers are the same as Algorithm 3. The performance of asynchronous Prox-MSVRG⁺⁺ is summarized as follows.

Theorem 4. *If $f(x)$ is convex and the domain Ω of x is bounded by D as in Corollary 1 (b). Suppose Assumptions 1, 3, 4 hold. Let $\theta_s = 2/(s + 2)$, $\eta_s = 1/(\sigma L\theta_s)$, where $\sigma > 100$. If delay $\tau < \frac{\sqrt{(1/\theta_s+2)^2+4(\sigma-1)}-(1/\theta_s+2)}{2}$, then under asynchronous Prox-MSVRG⁺⁺,*

$$\mathbf{E}[F(\tilde{x}^S) - F(x^*)] \leq \tilde{O}((L/m + LD/b)/S^2).$$

To the best of our knowledge, this is the first analysis for momentum accelerated asynchronous Proximal SVRG without strong convexity or sparsity assumptions. We obtain an $\tilde{O}(\frac{1}{\sqrt{\epsilon}})$ complexity, which improves upon the $O(\frac{1}{\epsilon})$ of Theorem 3. Note that the upper bound of τ is decreasing. From the theory perspective, this is consistent with the view that momentum acceleration requires accurate gradients [2, 13]. In other words, momentum methods may require a smaller delay in gradient computation.

We show in the following Corollary 3 that by choosing an increasing mini-batch size, we can loose the upper bound of τ . Moreover, our experiments with real-world data in Section 8 also show that Prox-MSVRG⁺⁺ achieves a remarkable acceleration.

Corollary 3. *If $b = \min\{s, n^{\frac{2}{3}}\}$, and the delay τ satisfies $\tau \leq \frac{\sqrt{9+4(\sigma-1)}-3}{2}$ (does not have to decrease), then*

$$\mathbf{E}[F(\tilde{x}^S) - F(x^*)] \leq 4\Delta/S^2 + 2\sigma L\Gamma/(mS^2) + 2LD \log S/(\tau S^2), \quad \text{where } S \leq n^{\frac{2}{3}}. \quad (7)$$

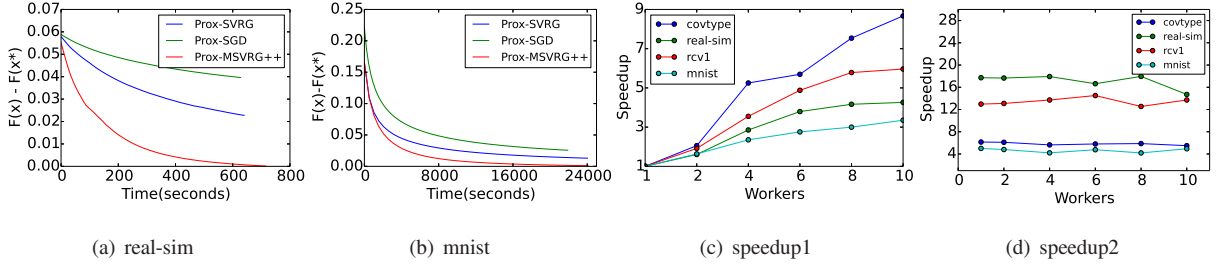


Figure 1: Figure (a) and (b) show the training curves of three algorithms on datasets *real-sim* and *mnist* using 4 workers. Figure (c) shows the speedups of Prox-MSVRG⁺⁺ and (d) shows the speedups of Prox-MSVRG⁺⁺ over Prox-SVRG with different numbers of workers.

8 Evaluation

In this section, we conduct experiments to evaluate the convergence rates and speedup properties of our algorithms. We evaluate K -class logistic regression [46] on real-world datasets including *covtype*, *real-sim*, *rcv1* and *mnist* from LibSVM [5], where *mnist* is a big multi-class dataset (Please see Supplementary Material for experimental details about the datasets). To demonstrate the comparisons clearly, we plot training curves near the optimal solution (truncate near the end). Three asynchronous algorithms are compared, i.e., Prox-MSVRG⁺⁺ (Section 7), Prox-SVRG (Section 6) and Prox-SGD (simply replace u_t^s in asynchronous Prox-SVRG to $\nabla f_{I_t^s}(x_{D(t)}^s)$).

Experimental Setup. We configure an experimental environment in a cluster with 11 physical machines. Each machine has 16 cores and 16GB memory. The communication among machines are handled by OpenMPI.² We use a constant step size for Prox-SVRG (Section 6) and a diminishing step size $\eta/(1+s)^\beta$ for Prox-SGD where $\eta, \beta \in (0, 1)$. The step size for Prox-MSVRG⁺⁺ is set according to Section 7. Moreover, the step size used for each algorithm is tuned to achieve the best results. We normalize the feature vector as in work [36].

Figure 1(a) and 1(b) depict the convergence of objective versus time of three algorithms using 4 workers, where x^* is obtained by running serial Prox-SVRG [43] until convergence (similar to [37]). It can be seen that Prox-MSVRG⁺⁺ has a faster convergence rate than Prox-SVRG and Prox-SGD in the asynchronous setting.

Next, we evaluate the speedup property of Prox-MSVRG⁺⁺ with different numbers of workers in Figure 1(c). The speedup of N workers is defined as the ratio of the time consumed by serial Prox-MSVRG⁺⁺ to that under using N workers (for achieving the same loss). The experimental results on 4 datasets show a significant speedup of Prox-MSVRG⁺⁺ when increasing the number of workers.

To precisely measure the acceleration efficiency, we plot the speedup of Prox-MSVRG⁺⁺ over Prox-SVRG with different numbers of workers in Figure 1(d), which equals the ratio of time consumed by Prox-SVRG to that of Prox-MSVRG⁺⁺ (both with the same number of workers). It can be seen that Prox-MSVRG⁺⁺ has remarkable improvements upon Prox-SVRG.

9 Conclusion

We develop a novel analysis for SVRG based proximal methods and their momentum acceleration for nonsmooth composite optimization. Through Prox-SVRG⁺⁺, we show that a linear rate can also be attained when the epoch length is chosen to be smaller than the condition number of the objective, and obtain a complexity of $O(n + LD/\epsilon)$ when the problem domain is bounded. Then, we change the beginning value of each epoch in Prox-SVRG⁺⁺ to develop Prox-MSVRG⁺⁺ and prove that it has a complexity of $O(1/\sqrt{\epsilon})$. To satisfy the need of large scale parallel computing, we further develop two asynchronous versions of SVRG based proximal methods, both with and without momentum. We present a new analysis under mild conditions, i.e. removing strong convexity and sparsity assumptions. Specifically, we consider a nonconvex objective in the analysis of the non-momentum accelerated asynchronous Prox-SVRG. The theoretical results show that a remarkable speedup can be achieved. Finally, we present experimental results to validate our theoretical findings.

²We use the communication framework of code in <https://github.com/slowbull/MPIPlatform>

References

- [1] A. Agarwal and J. C. Duchi. Distributed delayed stochastic optimization. In *Advances in Neural Information Processing Systems*, pages 873–881, 2011.
- [2] Z. Allen-Zhu. Katyusha: The first direct acceleration of stochastic gradient methods. *arXiv preprint arXiv:1603.05953*, 2016.
- [3] Z. Allen-Zhu and E. Hazan. Variance reduction for faster non-convex optimization. In *International Conference on Machine Learning*, pages 699–707, 2016.
- [4] Z. Allen-Zhu and Y. Yuan. Improved svrg for non-strongly-convex or sum-of-non-convex objectives. In *International conference on machine learning*, pages 1080–1089, 2016.
- [5] C.-C. Chang and C.-J. Lin. Libsvm : a library for support vector machines. *ACM Transactions on Intelligent Systems and Technology*, pages 2:27:1–27:27, 2011.
- [6] J. Dean, G. Corrado, R. Monga, K. Chen, M. Devin, M. Mao, A. Senior, P. Tucker, K. Yang, Q. V. Le, et al. Large scale distributed deep networks. In *Advances in neural information processing systems*, pages 1223–1231, 2012.
- [7] A. Defazio, F. Bach, and S. Lacoste-Julien. Saga: A fast incremental gradient method with support for non-strongly convex composite objectives. In *Advances in Neural Information Processing Systems*, pages 1646–1654, 2014.
- [8] S. Ghadimi, G. Lan, and H. Zhang. Mini-batch stochastic approximation methods for nonconvex stochastic composite optimization. *Mathematical Programming*, 155(1-2):267–305, 2016.
- [9] B. Gu, Z. Huo, and H. Huang. Asynchronous doubly stochastic group regularized learning. In *International Conference on Artificial Intelligence and Statistics*, pages 1791–1800, 2018.
- [10] L. T. K. Hien, C. Lu, H. Xu, and J. Feng. Accelerated stochastic mirror descent algorithms for composite non-strongly convex optimization. *arXiv preprint arXiv:1605.06892*, 2016.
- [11] Z. Huo and H. Huang. Asynchronous stochastic gradient descent with variance reduction for non-convex optimization. *arXiv preprint arXiv:1604.03584*, 2016.
- [12] R. Johnson and T. Zhang. Accelerating stochastic gradient descent using predictive variance reduction. In *Advances in neural information processing systems*, pages 315–323, 2013.
- [13] J. Konečný, J. Liu, P. Richtárik, and M. Takáč. Mini-batch semi-stochastic gradient descent in the proximal setting. *IEEE Journal of Selected Topics in Signal Processing*, 10(2):242–255, 2016.
- [14] G. Lan. An optimal method for stochastic composite optimization. *Mathematical Programming*, 133(1-2):365–397, 2012.
- [15] R. Leblond, F. Pedregosa, and S. Lacoste-Julien. Asaga: asynchronous parallel saga. *arXiv preprint arXiv:1606.04809*, 2016.
- [16] S.-I. Lee, H. Lee, P. Abbeel, and A. Y. Ng. Efficient Γ 1 regularized logistic regression. In *AAAI*, volume 6, pages 401–408, 2006.
- [17] L. Lei and M. I. Jordan. Less than a single pass: Stochastically controlled stochastic gradient method. *arXiv preprint arXiv:1609.03261*, 2016.
- [18] M. Li, D. G. Andersen, J. W. Park, A. J. Smola, A. Ahmed, V. Josifovski, J. Long, E. J. Shekita, and B.-Y. Su. Scaling distributed machine learning with the parameter server. In *OSDI*, volume 1, page 3, 2014.
- [19] M. Li, L. Zhou, Z. Yang, A. Li, F. Xia, D. G. Andersen, and A. Smola. Parameter server for distributed machine learning. In *Big Learning NIPS Workshop*, volume 6, page 2, 2013.

- [20] X. Lian, Y. Huang, Y. Li, and J. Liu. Asynchronous parallel stochastic gradient for nonconvex optimization. In *Advances in Neural Information Processing Systems*, pages 2737–2745, 2015.
- [21] H. Lin, J. Mairal, and Z. Harchaoui. A universal catalyst for first-order optimization. In *Advances in Neural Information Processing Systems*, pages 3384–3392, 2015.
- [22] Q. Lin, Z. Lu, and L. Xiao. An accelerated proximal coordinate gradient method. In *Advances in Neural Information Processing Systems*, pages 3059–3067, 2014.
- [23] J. Liu and S. J. Wright. Asynchronous stochastic coordinate descent: Parallelism and convergence properties. *SIAM Journal on Optimization*, 25(1):351–376, 2015.
- [24] J. Mairal. Incremental majorization-minimization optimization with application to large-scale machine learning. *SIAM Journal on Optimization*, 25(2):829–855, 2015.
- [25] H. Mania, X. Pan, D. Papailiopoulos, B. Recht, K. Ramchandran, and M. I. Jordan. Perturbed iterate analysis for asynchronous stochastic optimization. *arXiv preprint arXiv:1507.06970*, 2015.
- [26] Q. Meng, W. Chen, J. Yu, T. Wang, Z. Ma, and T.-Y. Liu. Asynchronous accelerated stochastic gradient descent. In *IJCAI*, pages 1853–1859, 2016.
- [27] Q. Meng, W. Chen, J. Yu, T. Wang, Z. Ma, and T.-Y. Liu. Asynchronous stochastic proximal optimization algorithms with variance reduction. In *AAAI*, pages 2329–2335, 2017.
- [28] J. J. Moreau. Fonctions convexes duales et points proximaux dans un espace hilbertien. *C.r.acad.sci.paris Ser.a Math*, 255:2897–2899, 1962.
- [29] Y. Nesterov. A method of solving a convex programming problem with convergence rate $o(1/k^2)$. In *Soviet Mathematics Doklady*, volume 27, pages 372–376, 1983.
- [30] Y. Nesterov. Smooth minimization of non-smooth functions. *Mathematical programming*, 103(1):127–152, 2005.
- [31] Y. Nesterov. *Introductory lectures on convex optimization: A basic course*, volume 87. Springer Science & Business Media, 2013.
- [32] A. Nitanda. Accelerated stochastic gradient descent for minimizing finite sums. In *Artificial Intelligence and Statistics*, pages 195–203, 2016.
- [33] C. Z. H. Qian and Z. S. T. Zhou. Accelerated stochastic admm for empirical risk minimization. *arXiv preprint arXiv:1611.04074*, 2016.
- [34] B. Recht, C. Re, S. Wright, and F. Niu. Hogwild: A lock-free approach to parallelizing stochastic gradient descent. In *Advances in neural information processing systems*, pages 693–701, 2011.
- [35] S. J. Reddi, A. Hefny, S. Sra, B. Póczos, and A. Smola. Stochastic variance reduction for nonconvex optimization. In *International conference on machine learning*, pages 314–323, 2016.
- [36] S. J. Reddi, A. Hefny, S. Sra, B. Póczos, and A. J. Smola. On variance reduction in stochastic gradient descent and its asynchronous variants. In *Advances in Neural Information Processing Systems*, pages 2647–2655, 2015.
- [37] S. J. Reddi, S. Sra, B. Póczos, and A. Smola. Fast stochastic methods for nonsmooth nonconvex optimization. In *Advances in Neural Information Processing Systems*, 2016.
- [38] R. T. Rockafellar. Monotone operators and the proximal point algorithm. *Siam Journal on Control and Optimization*, 14:877–898, 1976.
- [39] M. Schmidt, N. Le Roux, and F. Bach. Minimizing finite sums with the stochastic average gradient. In *Advances in Neural Information Processing Systems*, 2012.
- [40] F. Shang, Y. Liu, J. Cheng, and J. Zhuo. Fast stochastic variance reduced gradient method with momentum acceleration for machine learning. *arXiv preprint arXiv:1703.07948*, 2017.

- [41] F. Shang, K. Zhou, J. Cheng, I. W. Tsang, L. Zhang, and D. Tao. Vr-sgd: A simple stochastic variance reduction method for machine learning. *arXiv preprint arXiv:1802.09932*, 2018.
- [42] S. Sra. Scalable nonconvex inexact proximal splitting. *Advances in Neural Information Processing Systems*, pages 539–547, 2012.
- [43] L. Xiao and T. Zhang. A proximal stochastic gradient method with progressive variance reduction. *SIAM Journal on Optimization*, 24(4):2057–2075, 2014.
- [44] Y. Yu and L. Huang. Fast stochastic variance reduced admm for stochastic composition optimization. In *IJCAI*, pages 3364–3370, 2017.
- [45] L. Zhang, M. Mahdavi, and R. Jin. Linear convergence with condition number independent access of full gradients. In *Advances in Neural Information Processing Systems*, pages 980–988, 2013.
- [46] R. Zhang, S. Zheng, and J. T. Kwok. Asynchronous distributed semi-stochastic gradient optimization. *arXiv preprint arXiv:1508.01633*, 2015.
- [47] S. Zhang, A. E. Choromanska, and Y. LeCun. Deep learning with elastic averaging sgd. In *Advances in Neural Information Processing Systems*, pages 685–693, 2015.
- [48] S.-Y. Zhao, G.-D. Zhang, and W.-J. Li. Lock-free optimization for non-convex problems. In *AAAI*, pages 2935–2941, 2017.
- [49] S. Zheng and J. T. Kwok. Fast-and-light stochastic admm. *arXiv preprint arXiv:1604.07070v1*, 2016.
- [50] S. Zheng and J. T. Kwok. Fast-and-light stochastic admm. In *IJCAI*, pages 2407–2613, 2016.

Supplementary Material

In this section, we first present the comparison of Prox-MSVRG⁺⁺ with closely related accelerated algorithms. Then, we provide additional experimental results. After that, we present the full proofs of the theoretical results in the paper.

10 Comparison between Prox-MSVRG⁺⁺ and Related Algorithms

In Table 1, we summarize the gradient complexity and numbers of auxiliary variables of several closely related acceleration algorithms. It can be seen that Prox-MSVRG⁺⁺ achieves a lower complexity with less auxiliary variables.

Table 1: Comparison of acceleration algorithms including Katyusha^{ns} [2], Catalyst [21], AMSVRG [32], ASMD [10], APCG [22] for non-strongly convex objective. The abbreviation ‘AVs’ stands for “auxiliary variables”.

Algorithm	Gradient complexity	# of AVs
Prox-MSVRG ⁺⁺	$O(\max\{n, \sqrt{Ln}\} \frac{1}{\sqrt{\epsilon}})$	1
Katyusha ^{ns}	$O(\max\{n, \sqrt{Ln}\} \frac{1}{\sqrt{\epsilon}})$	2
Catalyst	$\tilde{O}(\frac{nL}{\sqrt{\epsilon}})$	1
AMSVRG	$O((n + \frac{nL}{\epsilon n + \sqrt{\epsilon L}}) \log \frac{1}{\epsilon})$	2
ASMD	$O(\max\{n, \sqrt{Ln}\} \frac{1}{\sqrt{\epsilon}})$	2
APCG	$O(\frac{n\sqrt{L}}{\sqrt{\epsilon}})$	2

11 Experimental Details and Additional Results

In this section, we first provide implementation details of our experiments. Then, we show additional experimental results.

11.1 Experimental Details

We use four real world datasets from LibSVM website³, including *rcv1*, *real-sim*, *covtype* and *mnist*. Details and experiment parameters about these four datasets are shown in Table 2. For binary class datasets, we use L_1 and L_2 regularizers, and adopt L_2 and nuclear norm for multi-class dataset, their corresponding weights can also be found in Table 2.

Table 2: Experimental details about datasets including *rcv1*, *real-sim*, *covtype*, *mnist*.

dataset	# of samples	# of features	# of classes	size of b	size of m	L_1 norm	L_2 norm	nuclear norm
rcv1	20,242	47,236	2	100	1000	10^{-5}	10^{-4}	\
real-sim	72,309	20,958	2	100	1000	10^{-4}	10^{-4}	\
covtype	581,012	54	2	100	1000	10^{-4}	10^{-4}	\
mnist	1,000,000	784	10	1500	2000	\	10^{-4}	10^{-5}

11.2 Additional Experiment Results

In this section, we provide additional experimental studies. We evaluate three asynchronous algorithms (the same as Section 8), including Prox-MSVRG⁺⁺ (Section 7), Prox-SVRG (Section 6) and Prox-SGD (simply replace u_i^s in asynchronous Prox-SVRG to $\nabla f_{I_t^s}(x_{D(t)}^s)$). Figure 2 shows the convergence of objective versus time, using 4 workers.

³<https://www.csie.ntu.edu.tw/~cjlin/libsvmtools/datasets/>

To demonstrate the comparisons clearly, we also plot training curves near the optimal solution (truncate near the end). The parameters and x^* are set according to the same rules in Section 8 in the submitted manuscript. It can be seen that Prox-MSVRG⁺⁺ outperforms the other two algorithms in our experiments.

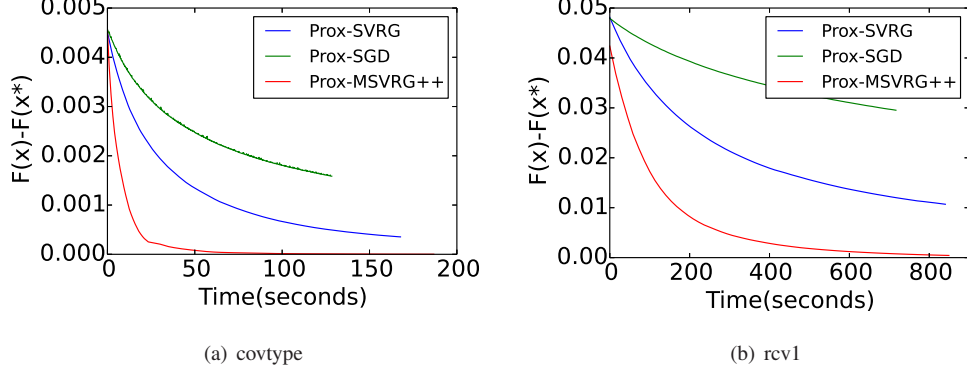


Figure 2: The training curves of three asynchronous algorithms, including Prox-SVRG⁺⁺, Prox-SVRG and Prox-SGD on datasets *covtype* and *rcv1*. The experiments are conducted over 4 workers.

12 Proofs of the Serial Algorithms

In this section, we provide the full proofs of Theorems 1, 2 and Corollaries 1, 2 for the serial algorithms, where the proof techniques in [40] are adopted. We first have the following result from [31] regarding the Lipschitz smooth property of $f(x)$, which will be used in our later analysis.

Lemma 1. *If $f_i(x)$ is L -Lipschitz smooth with positive constant $L > 0$, i.e., $\|\nabla f_i(x) - \nabla f_i(y)\| \leq L\|x - y\|$, then the following inequalities hold [31].*

$$f_i(y) \leq f_i(x) + \langle \nabla f_i(x), y - x \rangle + \frac{L}{2}\|x - y\|^2, \quad (8)$$

$$\langle \nabla f_i(x) - \nabla f_i(y), x - y \rangle \leq L\|x - y\|^2, \quad (9)$$

$$f_i(y) \geq f_i(x) + \langle \nabla f_i(x), y - x \rangle + \frac{1}{2L}\|\nabla f_i(x) - \nabla f_i(y)\|^2. \quad (10)$$

The following lemma is a widely used technical result in composite optimization, which is called *3-Point-Property*. Lemma 1 in [14] provides its detailed proofs and extensions.

Lemma 2. *If y_k^s is the optimal solution of*

$$\min_{y \in \mathcal{X}} \phi(y) + \frac{1}{2\eta_s}\|y - y_{k-1}^s\|^2, \quad (11)$$

where function $\phi(y)$ is convex over a convex set \mathcal{X} . Then for any $y \in \mathcal{X}$, we have [14]

$$\phi(y) + \frac{1}{2\eta_s}\|y - y_{k-1}^s\|^2 \geq \phi(y_k^s) + \frac{1}{2\eta_s}\|y_k^s - y_{k-1}^s\|^2 + \frac{1}{2\eta_s}\|y - y_k^s\|^2. \quad (12)$$

12.1 Proof of Theorem 1

Proof. Since $y_k^s = \text{prox}_{\eta_s h}(y_{k-1}^s - \eta_s \tilde{\nabla} f_{I_k^s}(x_{k-1}^s))$, we have from the definition of proximal operator that

$$y_k^s = \arg \min_y h(y) + \langle \tilde{\nabla} f_{I_k^s}(x_{k-1}^s), y - y_{k-1}^s \rangle + \frac{1}{2\eta_s}\|y - y_{k-1}^s\|^2. \quad (13)$$

Using Lemma 2 with $\phi(y) = h(y) + \langle \tilde{\nabla} f_{I_k^s}(x_{k-1}^s), y - y_{k-1}^s \rangle$ and $y = x^*$, we have

$$\begin{aligned} h(y_k^s) + \langle \tilde{\nabla} f_{I_k^s}(x_{k-1}^s), y_k^s - y_{k-1}^s \rangle &\leq h(x^*) + \langle \tilde{\nabla} f_{I_k^s}(x_{k-1}^s), x^* - y_{k-1}^s \rangle + \frac{1}{2\eta_s} \|x^* - y_{k-1}^s\|^2 \\ &\quad - \frac{1}{2\eta_s} \|y_k^s - y_{k-1}^s\|^2 - \frac{1}{2\eta_s} \|x^* - y_k^s\|^2. \end{aligned} \quad (14)$$

Since $f(x)$ is Lipschitz smooth, we obtain

$$\mathbf{E}f(x_k^s) \leq \mathbf{E}\left(f(x_{k-1}^s) + \langle \nabla f(x_{k-1}^s), x_k^s - x_{k-1}^s \rangle + \frac{L}{2} \|x_k^s - x_{k-1}^s\|^2\right). \quad (15)$$

Therefore,

$$\begin{aligned} \mathbf{E}F(x_k^s) &= \mathbf{E}\left(f(x_k^s) + h(x_k^s)\right) \\ &\leq \mathbf{E}\left(f(x_{k-1}^s) + \langle \nabla f(x_{k-1}^s), x_k^s - x_{k-1}^s \rangle + \frac{L}{2} \|x_k^s - x_{k-1}^s\|^2 + h(x_k^s)\right) \\ &\leq \mathbf{E}\left(f(x_{k-1}^s) + \langle \nabla f(x_{k-1}^s), x_k^s - x_{k-1}^s \rangle + \frac{L}{2} \|x_k^s - x_{k-1}^s\|^2 + \theta_s h(y_k^s) + (1 - \theta_s)h(\tilde{x}^{s-1})\right) \\ &= \mathbf{E}\left(f(x_{k-1}^s) + \langle \tilde{\nabla} f_{I_k^s}(x_{k-1}^s), \theta_s(y_k^s - y_{k-1}^s) \rangle + \frac{L}{2} \|x_k^s - x_{k-1}^s\|^2 + \theta_s h(y_k^s) + (1 - \theta_s)h(\tilde{x}^{s-1})\right. \\ &\quad \left. + \langle \nabla f(x_{k-1}^s) - \tilde{\nabla} f_{I_k^s}(x_{k-1}^s), \theta_s(y_k^s - y_{k-1}^s) \rangle\right) \\ &\leq \mathbf{E}\left(\theta_s h(x^*) + \underbrace{\langle \tilde{\nabla} f_{I_k^s}(x_{k-1}^s), \theta_s(x^* - y_{k-1}^s) \rangle}_{T_1} + \frac{\theta_s}{2\eta_s} \|x^* - y_{k-1}^s\|^2 - \frac{\theta_s}{2\eta_s} \|x^* - y_k^s\|^2 - \frac{\theta_s}{2\eta_s} \|y_k^s - y_{k-1}^s\|^2\right. \\ &\quad \left. + (1 - \theta_s)h(\tilde{x}^{s-1}) + f(x_{k-1}^s) + \frac{L}{2} \|x_k^s - x_{k-1}^s\|^2 + \underbrace{\langle \nabla f(x_{k-1}^s) - \tilde{\nabla} f_{I_k^s}(x_{k-1}^s), \theta_s(y_k^s - y_{k-1}^s) \rangle}_{T_2}\right), \end{aligned} \quad (16)$$

where we use $x_k^s = \theta_s y_k^s + (1 - \theta_s)\tilde{x}^{s-1}$ and the convexity of function $h(x)$ in the second inequality. The second equality comes from $x_k^s - x_{k-1}^s = \theta_s(y_k^s - y_{k-1}^s)$ and we adopt (14) in the final inequality.

We first bound T_1 as follows.

$$\begin{aligned} \mathbf{E}T_1 &= \mathbf{E}\langle \tilde{\nabla} f_{I_k^s}(x_{k-1}^s), \theta_s(x^* - y_{k-1}^s) \rangle \\ &= \mathbf{E}\langle \tilde{\nabla} f_{I_k^s}(x_{k-1}^s), \theta_s x^* + (1 - \theta_s)\tilde{x}^{s-1} - x_{k-1}^s \rangle \\ &= \mathbf{E}\langle \nabla f(x_{k-1}^s), \theta_s x^* + (1 - \theta_s)\tilde{x}^{s-1} - x_{k-1}^s \rangle, \end{aligned} \quad (17)$$

where we use $x_{k-1}^s = \theta_s y_{k-1}^s + (1 - \theta_s)\tilde{x}^{s-1}$ and that $\tilde{\nabla} f_{I_k^s}(x_{k-1}^s)$ is unbiased. Denote $\tilde{\nabla} f_{i_k^s}(x_{k-1}^s) = \nabla f_{i_k^s}(x_{k-1}^s) - \nabla f_{i_k^s}(\tilde{x}^{s-1}) + \tilde{\mu}$, where $i_k^s \in I_k^s$. Then, T_2 can be bounded as

$$\begin{aligned} \mathbf{E}T_2 &= \mathbf{E}\langle \nabla f(x_{k-1}^s) - \tilde{\nabla} f_{I_k^s}(x_{k-1}^s), \theta_s(y_k^s - y_{k-1}^s) \rangle \\ &\leq \frac{1}{2L} \mathbf{E}\|\nabla f(x_{k-1}^s) - \tilde{\nabla} f_{I_k^s}(x_{k-1}^s)\|^2 + \frac{L\theta_s^2}{2} \mathbf{E}\|y_k^s - y_{k-1}^s\|^2 \\ &\leq \frac{\rho(b)}{2L} \mathbf{E}\|\tilde{\nabla} f_{i_k^s}(x_{k-1}^s) - \nabla f(x_{k-1}^s)\|^2 + \frac{L\theta_s^2}{2} \mathbf{E}\|y_k^s - y_{k-1}^s\|^2 \\ &\leq \frac{\rho(b)}{2L} \mathbf{E}\|\nabla f_{i_k^s}(x_{k-1}^s) - \nabla f_{i_k^s}(\tilde{x}^{s-1})\|^2 + \frac{L\theta_s^2}{2} \mathbf{E}\|y_k^s - y_{k-1}^s\|^2 \\ &\leq \rho(b) \mathbf{E}\left(f(\tilde{x}^{s-1}) - f(x_{k-1}^s) - \langle \nabla f(x_{k-1}^s), \tilde{x}^{s-1} - x_{k-1}^s \rangle\right) + \frac{L\theta_s^2}{2} \mathbf{E}\|y_k^s - y_{k-1}^s\|^2, \end{aligned} \quad (18)$$

where $\rho(b) \triangleq \frac{n-b}{b(n-1)}$. Here the first inequality comes from Young's inequality and the the second inequality follows from Equation (15) in [49] (version v_1 , which is a technical report of [50]). In the third inequality, we use $\mathbf{E}\|x -$

$\mathbf{E}x\|^2 \leq \mathbf{E}\|x\|^2$. The last inequality follows from the Lipschitz smooth condition (10) of $f_i(x)$. Substituting (17) and (18) into (16), we get

$$\begin{aligned} \mathbf{E}F(x_k^s) &\leq \mathbf{E}\left(\theta_s h(x^*) + \frac{\theta_s}{2\eta_s}\|x^* - y_{k-1}^s\|^2 - \frac{\theta_s}{2\eta_s}\|x^* - y_k^s\|^2 - \frac{\theta_s}{2\eta_s}\|y_k^s - y_{k-1}^s\|^2\right. \\ &\quad \left.+ (1 - \theta_s)h(\tilde{x}^{s-1}) + f(x_{k-1}^s) + L\theta_s^2\|y_k^s - y_{k-1}^s\|^2\right. \\ &\quad \left.+ \rho(b)(f(\tilde{x}^{s-1}) - f(x_{k-1}^s)) - \underbrace{\rho(b)\langle \nabla f(x_{k-1}^s), \tilde{x}^{s-1} - x_{k-1}^s \rangle + \langle \nabla f(x_{k-1}^s), \theta_s x^* + (1 - \theta_s)\tilde{x}^{s-1} - x_{k-1}^s \rangle}_{T_4}\right). \end{aligned} \quad (19)$$

Because $f(x)$ is convex, if $1 - \theta_s - \rho(b) \geq 0$, then

$$\begin{aligned} T_4 &= \langle \nabla f(x_{k-1}^s), \theta_s x^* + (1 - \theta_s - \rho(b))\tilde{x}^{s-1} + \rho(b)x_{k-1}^s - x_{k-1}^s \rangle \\ &\leq f\left(\theta_s x^* + (1 - \theta_s - \rho(b))\tilde{x}^{s-1} + \rho(b)x_{k-1}^s\right) - f(x_{k-1}^s) \\ &\leq \theta_s f(x^*) + (1 - \theta_s - \rho(b))f(\tilde{x}^{s-1}) + \rho(b)f(x_{k-1}^s) - f(x_{k-1}^s). \end{aligned} \quad (20)$$

Putting it back into (19), we obtain that

$$\begin{aligned} \mathbf{E}F(x_k^s) &\leq \mathbf{E}\left((1 - \theta_s)F(\tilde{x}^{s-1}) + \theta_s F(x^*) + \frac{\theta_s}{2\eta_s}\|x^* - y_{k-1}^s\|^2 - \frac{\theta_s}{2\eta_s}\|x^* - y_k^s\|^2\right. \\ &\quad \left.- \frac{\theta_s}{2\eta_s}\|y_k^s - y_{k-1}^s\|^2 + L\theta_s^2\|y_k^s - y_{k-1}^s\|^2\right) \\ &= \mathbf{E}\left((1 - \theta_s)F(\tilde{x}^{s-1}) + \theta_s F(x^*) + L\theta_s^2\|x^* - y_{k-1}^s\|^2 - L\theta_s^2\|x^* - y_k^s\|^2\right), \end{aligned} \quad (21)$$

where the second equality follows from $\eta_s = \frac{1}{2L\theta_s}$. Summing the above from $k = 1$ to m , and using $\tilde{x}^s = \frac{1}{m} \sum_{k=1}^m x_k^s$, we obtain

$$\mathbf{E}\left(F(\tilde{x}^s) - F(x^*)\right) \leq (1 - \theta_s)\mathbf{E}\left(F(\tilde{x}^{s-1}) - F(x^*)\right) + \frac{L\theta_s^2}{m}\mathbf{E}(\|y_0^s - x^*\|^2 - \|y_m^s - x^*\|^2). \quad (22)$$

□

12.2 Proof of Corollary 1

Proof of (a). If $F(x)$ is μ -strongly convex, then $\|y_0^s - x^*\|^2 = \|\tilde{x}^{s-1} - x^*\|^2 \leq \frac{2}{\mu}\left(F(\tilde{x}^{s-1}) - F(x^*)\right)$. Let $\theta_s \equiv \theta$ and $\eta_s \equiv \eta$. It follows from (22) that

$$\begin{aligned} \mathbf{E}\left(F(\tilde{x}^s) - F(x^*)\right) &\leq (1 - \theta)\mathbf{E}\left(F(\tilde{x}^{s-1}) - F(x^*)\right) + \frac{L\theta^2}{m}\mathbf{E}(\|y_0^s - x^*\|^2) \\ &\leq (1 - \theta + \frac{2\kappa}{m}\theta^2)\mathbf{E}\left(F(\tilde{x}^{s-1}) - F(x^*)\right). \end{aligned} \quad (23)$$

where $\kappa \triangleq \frac{L}{\mu}$ is the condition number of $F(x)$.

Proof of (a.1). Under conditions in Corollary 1(a.1), it can be verified that if $s \geq \lceil \log \frac{F(\tilde{x}^0) - F(x^*)}{\epsilon} \rceil / \log \frac{4}{3}$, $\mathbf{E}\left(F(\tilde{x}^s) - F(x^*)\right) \leq \epsilon$. From Algorithm 1 we know that the total number of gradients calculated in s epochs is $sn + smb$. We can choose a small b to satisfy $\theta + \rho(b) \leq 1$. Thus, the gradient complexity of Algorithm 1 is $O((n + \kappa) \log \frac{1}{\epsilon})$. Using the same arguments we obtain result in (a.2).

Proof of (b). If the domain of x is bounded by D , the possibility of going beyond the domain can be avoided by the proximal operator shown in Lemma 2. Then, we know from (22) that

$$\mathbf{E}\left(F(\tilde{x}^s) - F(x^*)\right) \leq (1 - \theta_s)\mathbf{E}\left(F(\tilde{x}^{s-1}) - F(x^*)\right) + \frac{L\theta_s^2 D}{m}. \quad (24)$$

Note that $\frac{1-\theta_s}{\theta_s^2} \leq \frac{1}{\theta_{s-1}^2}$ when $\theta_s = \frac{2}{s+2}$. Thus, setting $\theta_0 = 1$, dividing both sides of (24) by θ_s^2 , and summing over $s = 1$ to S , we finally obtain:

$$\mathbf{E}\left(F(\tilde{x}^S) - F(x^*)\right) \leq \frac{4(F(\tilde{x}^0) - F(x^*))}{S^2} + \frac{4LD}{mS}. \quad (25)$$

To derive the bound of gradient complexity, we can choose $b = \Theta(1)$ to satisfy $\rho(b) \leq 1 - \theta_s$ (actually we only need $b > 3$). Moreover, it can be obtained from Algorithm 1 that the total number of gradients calculated in S epochs is $Sn + Smb$. Also, for a large S , we have $\frac{4(F(\tilde{x}^0) - F(x^*))}{S^2} \leq \frac{4LD}{mS}$. Thus, by setting $S = \max\{1, \frac{8LD}{m\epsilon}\}$, we have $\mathbf{E}\left(F(\tilde{x}^S) - F(x^*)\right) \leq \epsilon$, and the resulting asymptotic gradient complexity equals $O(n + \frac{LD}{\epsilon})$ if $m = n$. \square

12.3 Proof of Theorem 2

Proof. Since we only change the initialization of x, y in each epoch, and the new x_0^s, y_0^s still satisfy Step 10 in Algorithm 1 when $k = 0$. Thus, several proof steps in section 12.1 still hold in this case. Following the proof of Theorem 1 (start from (13)), we can get (22). Using $y_0^s = y_m^{s-1}$, we have that

$$\mathbf{E}\left(F(\tilde{x}^s) - F(x^*)\right) \leq (1 - \theta_s)\mathbf{E}\left(F(\tilde{x}^{s-1}) - F(x^*)\right) + \frac{L\theta_s^2}{m}\mathbf{E}(\|y_m^{s-1} - x^*\|^2 - \|y_m^s - x^*\|^2). \quad (26)$$

Dividing both sides by θ_s^2 , summing up from $s = 1$ to S , and using $\frac{1-\theta_s}{\theta_s^2} \leq \frac{1}{\theta_{s-1}^2}$ when $\theta_s = \frac{2}{s+2}$, we obtain:

$$\mathbf{E}\left(F(\tilde{x}^S) - F(x^*)\right) \leq \frac{4(F(\tilde{x}^0) - F(x^*))}{S^2} + \frac{4L\|\tilde{x}^0 - x^*\|^2}{mS^2}. \quad (27)$$

This completes the proof. \square

12.4 Proof of Corollary 2

Proof. Similar to the proof of Corollary 1(b). Let $m = n, S = \max\{\sqrt{\frac{8(F(\tilde{x}^0) - F(x^*))}{\epsilon}}, \sqrt{\frac{8L\|\tilde{x}^0 - x^*\|^2}{m\epsilon}}\}$. It can be verified that the gradient complexity equals to $O(\max\{n, \sqrt{Ln}\} \frac{1}{\sqrt{\epsilon}})$. \square

13 Proofs of Asynchronous Algorithms

In this section, we present the proofs for Theorems 3, 4 and Corollary 3 for the asynchronous algorithms. Denote

$$\begin{aligned} u_t^s &= \frac{1}{|I_t^s|} \sum_{i_t^s \in I_t^s} \left(\nabla f_{i_t^s}(x_{D(t)}^s) - \nabla f_{i_t^s}(\tilde{x}^{s-1}) \right) + \nabla f(\tilde{x}^{s-1}), \\ v_t^s &= \frac{1}{|I_t^s|} \sum_{i_t^s \in I_t^s} \left(\nabla f_{i_t^s}(x_t^s) - \nabla f_{i_t^s}(\tilde{x}^{s-1}) \right) + \nabla f(\tilde{x}^{s-1}) \end{aligned} \quad (28)$$

and $\nabla f_{I_t^s}(x) = \frac{1}{|I_t^s|} \sum_{i_t^s \in I_t^s} \nabla f_{i_t^s}(x)$ for simplicity of notation. We see that v_t^s is the un-delayed variance reduced gradient. Define $\bar{x}_{t+1}^s = \text{prox}_{\eta h}(x_t^s - \eta \nabla f(x_t^s))$. From the submitted manuscript we know that the *gradient mapping* term $G_\eta(x) = \frac{1}{\eta}[x - \text{prox}_{\eta h}(x - \eta \nabla f(x))]$ is used to measure convergence property in this nonconvex proximal setting. Therefore, we only need to find a point x that satisfies $\|G_\eta(x)\|^2 \leq \epsilon$. Moreover, from the above definition we have $G_\eta(x_t^s) = \frac{1}{\eta}[x_t^s - \text{prox}_{\eta h}(x_t^s - \eta \nabla f(x_t^s))] = \frac{1}{\eta}(x_t^s - \bar{x}_{t+1}^s)$.

13.1 Proof of Theorem 3

We analyze the convergence of Algorithm 3 in this section, where a proof technique of Lyapunov function in [37] is adopted.

Proof. Since $x_{t+1}^s = \text{prox}_{\eta h}(x_t^s - \eta u_t^s)$, applying Lemma 2 in [37], for any $z \in R^d$, we have

$$F(x_{t+1}^s) \leq F(z) + \langle x_{t+1}^s - z, \nabla f(x_t^s) - u_t^s \rangle + \left(\frac{L}{2} - \frac{1}{2\eta}\right) \|x_{t+1}^s - x_t^s\|^2 + \left(\frac{L}{2} + \frac{1}{2\eta}\right) \|z - x_t^s\|^2 - \frac{1}{2\eta} \|x_{t+1}^s - z\|^2. \quad (29)$$

Similarly, for $\bar{x}_{t+1}^s = \text{prox}_{\eta h}(x_t^s - \eta \nabla f(x_t^s))$, we obtain

$$F(\bar{x}_{t+1}^s) \leq F(z) + \left(\frac{L}{2} - \frac{1}{2\eta}\right) \|\bar{x}_{t+1}^s - x_t^s\|^2 + \left(\frac{L}{2} + \frac{1}{2\eta}\right) \|z - x_t^s\|^2 - \frac{1}{2\eta} \|\bar{x}_{t+1}^s - z\|^2, \quad \forall z \in R^d. \quad (30)$$

Letting $z = \bar{x}_{t+1}^s$ in (29) and $z = x_t^s$ in (30), summing them together, and taking expectations, we have

$$\mathbf{E}F(x_{t+1}^s) \leq \mathbf{E}\left(F(x_t^s) + \underbrace{\langle x_{t+1}^s - \bar{x}_{t+1}^s, \nabla f(x_t^s) - u_t^s \rangle}_{T_1} + \left(\frac{L}{2} - \frac{1}{2\eta}\right) \|x_{t+1}^s - x_t^s\|^2 + \left(L - \frac{1}{2\eta}\right) \|\bar{x}_{t+1}^s - x_t^s\|^2 - \frac{1}{2\eta} \|x_{t+1}^s - \bar{x}_{t+1}^s\|^2\right). \quad (31)$$

Using Young's Inequality, we see that

$$\begin{aligned} T_1 &= \langle x_{t+1}^s - \bar{x}_{t+1}^s, \nabla f(x_t^s) - u_t^s \rangle \\ &\leq \frac{1}{2\eta} \|x_{t+1}^s - \bar{x}_{t+1}^s\|^2 + \frac{\eta}{2} \|\nabla f(x_t^s) - u_t^s\|^2. \end{aligned} \quad (32)$$

Therefore,

$$\mathbf{E}F(x_{t+1}^s) \leq \mathbf{E}\left(F(x_t^s) + \frac{\eta}{2} \underbrace{\|\nabla f(x_t^s) - u_t^s\|^2}_{T_2} + \left(\frac{L}{2} - \frac{1}{2\eta}\right) \|x_{t+1}^s - x_t^s\|^2 + \left(L - \frac{1}{2\eta}\right) \|\bar{x}_{t+1}^s - x_t^s\|^2\right). \quad (33)$$

Next we bound T_2 . We have:

$$T_2 = \|\nabla f(x_t^s) - u_t^s\|^2 \leq 2 \underbrace{\|\nabla f(x_t^s) - v_t^s\|^2}_{T_3} + 2 \underbrace{\|v_t^s - u_t^s\|^2}_{T_4} \quad (34)$$

The term T_3 can be bounded as follows.

$$\begin{aligned} \mathbf{E}T_3 &= \mathbf{E}\|v_t^s - \nabla f(x_t^s)\|^2 \\ &\leq \rho(b) \mathbf{E}\|\nabla f_{i_t^s}(x_t^s) - \nabla f_{i_t^s}(\tilde{x}^{s-1}) + \nabla f(\tilde{x}^{s-1}) - \nabla f(x_t^s)\|^2 \\ &\leq \rho(b) \mathbf{E}\|\nabla f_{i_t^s}(x_t^s) - \nabla f_{i_t^s}(\tilde{x}^{s-1})\|^2 \\ &\leq L^2 \rho(b) \mathbf{E}\|x_t^s - \tilde{x}^{s-1}\|^2, \end{aligned} \quad (35)$$

where the first inequality results from Equation (15) in [49] (version *v1*, which is a technical report of [50]). The second inequality uses $\mathbf{E}\|x - \mathbf{E}x\|^2 \leq \mathbf{E}\|x\|^2$, and the third inequality follows from the Lipschitz smoothness property of $f_i(x)$. On the other hand, T_4 can be bounded as follows.

$$\begin{aligned} \mathbf{E}T_4 &= \mathbf{E}\|v_t^s - u_t^s\|^2 \\ &= \mathbf{E}\left\|\frac{1}{|I_t^s|} \sum_{i_t^s \in I_t^s} [\nabla f_{i_t^s}(x_t^s) - \nabla f_{i_t^s}(x_{D(t)}^s)]\right\|^2 \\ &\leq \frac{1}{b} \sum_{i_t^s \in I_t^s} \mathbf{E}\|\nabla f_{i_t^s}(x_t^s) - \nabla f_{i_t^s}(x_{D(t)}^s)\|^2 \\ &\leq L^2 \mathbf{E}\|x_t^s - x_{D(t)}^s\|^2 \\ &= L^2 \mathbf{E}\left\|\sum_{d=D(t)}^{t-1} (x_{d+1}^s - x_d^s)\right\|^2 \\ &\leq L^2 \tau \sum_{d=D(t)}^{t-1} \mathbf{E}\|x_{d+1}^s - x_d^s\|^2. \end{aligned} \quad (36)$$

Here the first and third inequality follow from $\|\sum_{i=1}^n a_i\|^2 \leq n \sum_{i=1}^n \|a_i\|^2$. The second inequality uses the Lipschitz smooth property of $f_i(x)$. Therefore, T_2 can be bounded as

$$\mathbf{E}T_2 \leq 2L^2\rho(b)\mathbf{E}\|x_t^s - \tilde{x}^{s-1}\|^2 + 2L^2\tau \sum_{d=D(t)}^{t-1} \mathbf{E}\|x_{d+1}^s - x_d^s\|^2. \quad (37)$$

Substituting (37) in (33), we obtain

$$\begin{aligned} \mathbf{E}F(x_{t+1}^s) &\leq \mathbf{E}\left(F(x_t^s) + \eta L^2\rho(b)\|x_t^s - \tilde{x}^{s-1}\|^2 + \eta L^2\tau \sum_{d=D(t)}^{t-1} \|x_{d+1}^s - x_d^s\|^2\right) \\ &\quad + \left(\frac{L}{2} - \frac{1}{2\eta}\right)\|x_{t+1}^s - x_t^s\|^2 + \left(L - \frac{1}{2\eta}\right)\|\bar{x}_{t+1}^s - x_t^s\|^2. \end{aligned} \quad (38)$$

Denote $R_t^s \triangleq \mathbf{E}\left(F(x_t^s) + c_t\|x_t^s - \tilde{x}^{s-1}\|^2\right)$, where $\{c_t\}_{t=0}^m$ is a decreasing sequence which satisfies $c_m = 0$ and $c_t = c_{t+1}(1 + \beta) + \eta L^2\rho(b)$. The value of β ($\beta > 0$) will be specified in the following. We have

$$\begin{aligned} R_{t+1}^s &= \mathbf{E}\left(F(x_{t+1}^s) + c_{t+1}\|x_{t+1}^s - \tilde{x}^{s-1}\|^2\right) \\ &\leq \mathbf{E}\left(F(x_{t+1}^s) + c_{t+1}\left(1 + \frac{1}{\beta}\right)\|x_{t+1}^s - x_t^s\|^2 + c_{t+1}(1 + \beta)\|x_t^s - \tilde{x}^{s-1}\|^2\right) \\ &\leq \mathbf{E}\left(F(x_t^s) + [c_{t+1}(1 + \beta) + \eta L^2\rho(b)]\|x_t^s - \tilde{x}^{s-1}\|^2 + \left[c_{t+1}\left(1 + \frac{1}{\beta}\right) + \frac{L}{2} - \frac{1}{2\eta}\right]\|x_{t+1}^s - x_t^s\|^2\right) \\ &\quad + \eta L^2\tau \sum_{d=D(t)}^{t-1} \|x_{d+1}^s - x_d^s\|^2 + \left[L - \frac{1}{2\eta}\right]\|x_t^s - \bar{x}_{t+1}^s\|^2. \end{aligned} \quad (39)$$

Summing it up from $t = 0$ to $m - 1$, since $\sum_{t=0}^{m-1} \sum_{d=D(t)}^{t-1} \|x_{d+1}^s - x_d^s\|^2 \leq \tau \sum_{t=0}^{m-1} \|x_{t+1}^s - x_t^s\|^2$, we obtain

$$\sum_{t=0}^{m-1} R_{t+1}^s \leq \sum_{t=0}^{m-1} R_t^s + \sum_{t=0}^{m-1} \left[c_{t+1}\left(1 + \frac{1}{\beta}\right) + \frac{L}{2} - \frac{1}{2\eta} + \eta L^2\tau^2 \right] \mathbf{E}\|x_{t+1}^s - x_t^s\|^2 + \sum_{t=0}^{m-1} \left[L - \frac{1}{2\eta} \right] \mathbf{E}\|x_t^s - \bar{x}_{t+1}^s\|^2. \quad (40)$$

Let $\beta = \frac{1}{m}$, now we want to deserve the constraint of τ that makes sure $c_{t+1}\left(1 + \frac{1}{\beta}\right) + \frac{L}{2} - \frac{1}{2\eta} + \eta L^2\tau^2 \leq 0$. From $c_m = 0$ and $c_t = c_{t+1}(1 + \beta) + \eta L^2\rho(b)$, we obtain the bound of c_0 as follows.

$$\begin{aligned} c_0 &= \eta L^2\rho(b) \frac{(1 + \beta)^m - 1}{\beta} \\ &= m\eta L^2\rho(b) \left[\left(1 + \frac{1}{m}\right)^m - 1 \right] \\ &\leq m\eta L^2\rho(b)(e - 1) \leq 2m\eta L^2\rho(b). \end{aligned} \quad (41)$$

Let $\eta = \frac{\sigma}{L}$, where $0 < \sigma < \frac{1}{3}$. In order to ensure $c_{t+1}\left(1 + \frac{1}{\beta}\right) + \frac{L}{2} - \frac{1}{2\eta} + \eta L^2\tau^2 \leq 0$, we only need $c_0\left(1 + \frac{1}{\beta}\right) + \frac{L}{2} - \frac{1}{2\eta} + \eta L^2\tau^2 \leq 0$, and it suffices to prove

$$\left(8m^2\rho(b) + 2\tau^2\right)\sigma^2 + \sigma - 1 \leq 0. \quad (42)$$

Because $\rho(b) = \frac{n-b}{b(n-1)} \leq \frac{1}{b}$, the above condition becomes

$$\left(\frac{8m^2}{b} + 2\tau^2\right)\sigma^2 + \sigma - 1 \leq 0. \quad (43)$$

Let $m = \lceil n^{\frac{1}{3}} \rceil$ and $b = \lceil 8n^{\frac{2}{3}} \rceil$, we have

$$(1 + 2\tau^2)\sigma^2 + \sigma - 1 \leq 0, \quad (44)$$

then we obtain the constraint $\tau^2 \leq \frac{1-\sigma-\sigma^2}{2\sigma^2}$. Suppose the delay bound τ and step size η satisfy this constraint, then Equation (40) becomes

$$\sum_{t=0}^{m-1} R_{t+1}^s \leq \sum_{t=0}^{m-1} R_t^s + \sum_{t=0}^{m-1} (L - \frac{1}{2\eta}) \mathbf{E} \|x_t^s - \bar{x}_{t+1}^s\|^2. \quad (45)$$

Since $\eta \leq \frac{1}{2L}$, we have

$$(\frac{1}{2\eta} - L) \sum_{t=0}^{m-1} \mathbf{E} \|x_t^s - \bar{x}_{t+1}^s\|^2 \leq R_0^s - R_m^s = \mathbf{E} [F(x_0^s) - F(x_m^s)] = \mathbf{E} [F(\tilde{x}^{s-1}) - F(\tilde{x}^s)]. \quad (46)$$

Summing the above inequality over $s = 1$ to S , we get

$$\frac{1}{T} (\frac{1}{2\eta} - L) \sum_{s=1}^S \sum_{t=0}^{m-1} \mathbf{E} \|x_t^s - \bar{x}_{t+1}^s\|^2 \leq \frac{1}{T} [F(\tilde{x}^0) - F(x^*)], \quad (47)$$

where x^* is the optimal solution. Substituting the convergence measurement $G_\eta(x_t^s) = \frac{1}{\eta}(x_t^s - \bar{x}_{t+1}^s)$, we finally obtain

$$\frac{1}{T} \sum_{s=1}^S \sum_{t=0}^{m-1} \mathbf{E} \|G_\eta(x_t^s)\|^2 \leq \frac{2L[F(\tilde{x}^0) - F(x^*)]}{T\sigma(1-2\sigma)}. \quad (48)$$

From Algorithm 3, we know that the total number of gradients calculated in S epochs is $Sn + Smb$. Now let $S = \frac{2L[F(\tilde{x}^0) - F(x^*)]}{m\sigma(1-2\sigma)\epsilon}$. Then, it can be verified that the gradient complexity equals to $O(n + \frac{Ln^{\frac{2}{3}}}{\epsilon})$. \square

13.2 Proof of Theorem 4

Proof. From the update rule of y_{t+1}^s , we know that

$$y_{t+1}^s = \arg \min_y h(y) + \langle u_t^s, y - y_t^s \rangle + \frac{1}{2\eta_s} \|y - y_t^s\|^2. \quad (49)$$

Applying Lemma 2 with $\phi(y) = h(y) + \langle u_t^s, y - y_t^s \rangle$ and $y = x^*$, we obtain

$$h(y_{t+1}^s) + \langle u_t^s, y_{t+1}^s - y_t^s \rangle \leq h(x^*) + \langle u_t^s, x^* - y_t^s \rangle + \frac{1}{2\eta_s} \|x^* - y_t^s\|^2 - \frac{1}{2\eta_s} \|x^* - y_{t+1}^s\|^2 - \frac{1}{2\eta_s} \|y_{t+1}^s - y_t^s\|^2. \quad (50)$$

Since $f(x)$ is Lipschitz smooth, we have

$$\begin{aligned} \mathbf{E} f(x_{t+1}^s) &\leq \mathbf{E} \left(f(x_t^s) + \langle \nabla f(x_t^s), x_{t+1}^s - x_t^s \rangle + \frac{L}{2} \|x_{t+1}^s - x_t^s\|^2 \right) \\ &= \mathbf{E} \left(f(x_t^s) + \theta_s \langle u_t^s, y_{t+1}^s - y_t^s \rangle + \theta_s \langle \nabla f(x_t^s) - u_t^s, y_{t+1}^s - y_t^s \rangle + \frac{L}{2} \|x_{t+1}^s - x_t^s\|^2 \right), \end{aligned} \quad (51)$$

where the second equality uses $x_{t+1}^s - x_t^s = \theta_s(y_{t+1}^s - y_t^s)$. Therefore,

$$\begin{aligned} \mathbf{E} F(x_{t+1}^s) &= \mathbf{E} [f(x_{t+1}^s) + h(x_{t+1}^s)] \\ &\leq \mathbf{E} \left[f(x_t^s) + \theta_s \langle u_t^s, y_{t+1}^s - y_t^s \rangle + \theta_s \langle \nabla f(x_t^s) - u_t^s, y_{t+1}^s - y_t^s \rangle + \frac{L}{2} \|x_{t+1}^s - x_t^s\|^2 + h(x_{t+1}^s) \right] \\ &\leq \mathbf{E} \left[f(x_t^s) + \theta_s \langle u_t^s, y_{t+1}^s - y_t^s \rangle + \theta_s \langle \nabla f(x_t^s) - u_t^s, y_{t+1}^s - y_t^s \rangle + \frac{L}{2} \|x_{t+1}^s - x_t^s\|^2 \right. \\ &\quad \left. + (1 - \theta_s)h(\tilde{x}^{s-1}) + \theta_s h(y_{t+1}^s) \right] \\ &\leq \mathbf{E} \left[\theta_s h(x^*) + \underbrace{\theta_s \langle u_t^s, x^* - y_t^s \rangle}_{T_1} + \frac{\theta_s}{2\eta_s} \|x^* - y_t^s\|^2 - \frac{\theta_s}{2\eta_s} \|x^* - y_{t+1}^s\|^2 - \frac{\theta_s}{2\eta_s} \|y_{t+1}^s - y_t^s\|^2 \right. \\ &\quad \left. + f(x_t^s) + \theta_s \langle \nabla f(x_t^s) - u_t^s, y_{t+1}^s - y_t^s \rangle + \frac{L}{2} \|x_{t+1}^s - x_t^s\|^2 + (1 - \theta_s)h(\tilde{x}^{s-1}) \right], \end{aligned} \quad (52)$$

where the first inequality uses (51), and the second inequality follows from $x_{t+1}^s = \theta_s y_{t+1}^s + (1 - \theta_s) \tilde{x}^{s-1}$ and the convexity of $h(x)$. We apply (50) in the third inequality. T_1 can be bounded as follows.

$$\begin{aligned}
\mathbf{E}T_1 &= \theta_s \mathbf{E}\langle u_t^s, x^* - y_t^s \rangle \\
&= \mathbf{E}\langle u_t^s, \theta_s x^* + (1 - \theta_s) \tilde{x}^{s-1} - x_t^s \rangle \\
&= \mathbf{E}\langle u_t^s, \theta_s x^* + (1 - \theta_s) \tilde{x}^{s-1} - x_{D(t)}^s \rangle + \mathbf{E}\langle u_t^s, x_{D(t)}^s - x_t^s \rangle \\
&= \mathbf{E}\langle \nabla f(x_{D(t)}^s), \theta_s x^* + (1 - \theta_s) \tilde{x}^{s-1} - x_{D(t)}^s \rangle + \mathbf{E}\langle \nabla f(x_{D(t)}^s), x_{D(t)}^s - x_t^s \rangle \\
&\leq \mathbf{E}\left[f(\theta_s x^* + (1 - \theta_s) \tilde{x}^{s-1}) - f(x_{D(t)}^s) + f(x_{D(t)}^s) - f(x_t^s) + \frac{L}{2} \|x_{D(t)}^s - x_t^s\|^2 \right] \\
&\leq \mathbf{E}\left[\theta_s f(x^*) + (1 - \theta_s) f(\tilde{x}^{s-1}) - f(x_t^s) + \frac{L}{2} \|x_{D(t)}^s - x_t^s\|^2 \right],
\end{aligned} \tag{53}$$

where the convexity and Lipschitz smoothness of $f(x)$ are adopted in the first inequality. Putting it back in Equation (52), we get

$$\begin{aligned}
\mathbf{E}F(x_{t+1}^s) &\leq \mathbf{E}\left[(1 - \theta_s)F(\tilde{x}^{s-1}) + \theta_s F(x^*) + \frac{\theta_s}{2\eta_s} (\|x^* - y_t^s\|^2 - \|x^* - y_{t+1}^s\|^2) + \frac{L}{2} \|x_{D(t)}^s - x_t^s\|^2 \right. \\
&\quad \left. + \frac{L}{2} \|x_{t+1}^s - x_t^s\|^2 - \frac{\theta_s}{2\eta_s} \|y_{t+1}^s - y_t^s\|^2 + \underbrace{\theta_s \langle \nabla f(x_t^s) - u_t^s, y_{t+1}^s - y_t^s \rangle}_{T_2} \right],
\end{aligned} \tag{54}$$

where

$$T_2 = \theta_s \langle \nabla f(x_t^s) - u_t^s, y_{t+1}^s - y_t^s \rangle = \underbrace{\theta_s \langle \nabla f(x_t^s) - v_t^s, y_{t+1}^s - y_t^s \rangle}_{T_3} + \underbrace{\theta_s \langle v_t^s - u_t^s, y_{t+1}^s - y_t^s \rangle}_{T_4}. \tag{55}$$

Next we bound T_3 and T_4 .

$$\begin{aligned}
\mathbf{E}T_3 &= \theta_s \mathbf{E}\langle \nabla f(x_t^s) - v_t^s, y_{t+1}^s - y_t^s \rangle \\
&\leq \frac{\theta_s}{2\tau L} \mathbf{E}\|\nabla f(x_t^s) - v_t^s\|^2 + \frac{\tau L \theta_s}{2} \mathbf{E}\|y_{t+1}^s - y_t^s\|^2 \\
&\leq \frac{\theta_s \rho(b)}{2\tau L} \mathbf{E}\|\nabla f_{i_t^s}(x_t^s) - \nabla f_{i_t^s}(\tilde{x}^{s-1}) + \nabla f(\tilde{x}^{s-1}) - \nabla f(x_t^s)\|^2 + \frac{\tau L \theta_s}{2} \mathbf{E}\|y_{t+1}^s - y_t^s\|^2 \\
&\leq \frac{\theta_s \rho(b)}{2\tau L} \mathbf{E}\|\nabla f_{i_t^s}(x_t^s) - \nabla f_{i_t^s}(\tilde{x}^{s-1})\|^2 + \frac{\tau L \theta_s}{2} \mathbf{E}\|y_{t+1}^s - y_t^s\|^2 \\
&\leq \frac{\theta_s \rho(b) L^2}{2\tau L} \mathbf{E}\|x_t^s - \tilde{x}^{s-1}\|^2 + \frac{\tau L \theta_s}{2} \mathbf{E}\|y_{t+1}^s - y_t^s\|^2 \\
&= \frac{\theta_s^3 \rho(b) L^2}{2\tau L} \mathbf{E}\|y_t^s - \tilde{x}^{s-1}\|^2 + \frac{\tau L \theta_s}{2} \mathbf{E}\|y_{t+1}^s - y_t^s\|^2 \\
&\leq \frac{\theta_s^3 \rho(b) L D}{2\tau} + \frac{\tau L \theta_s}{2} \mathbf{E}\|y_{t+1}^s - y_t^s\|^2,
\end{aligned} \tag{56}$$

where in the first inequality we use Young's inequality, and the second to the fourth inequality can be explained by the same arguments in (35). The second equality follows from $x_t^s - \tilde{x}^{s-1} = \theta_s(y_t^s - \tilde{x}^{s-1})$. Moreover,

$$\begin{aligned}
\mathbf{E}T_4 &= \theta_s \mathbf{E} \langle v_t^s - u_t^s, y_{t+1}^s - y_t^s \rangle \\
&= \theta_s \mathbf{E} \langle \nabla f_{I_t^s}(x_t^s) - \nabla f_{I_t^s}(x_{D(t)}^s), y_{t+1}^s - y_t^s \rangle \\
&\leq \theta_s L \mathbf{E} \|x_{D(t)}^s - x_t^s\| \|y_{t+1}^s - y_t^s\| \\
&= \theta_s L \mathbf{E} \left\| \sum_{d=D(t)}^{t-1} (x_d^s - x_{d+1}^s) \right\| \|y_{t+1}^s - y_t^s\| \\
&\leq \theta_s L \sum_{d=D(t)}^{t-1} \mathbf{E} \left[\|x_d^s - x_{d+1}^s\| \|y_{t+1}^s - y_t^s\| \right] \\
&\leq L \sum_{d=D(t)}^{t-1} \mathbf{E} \left[\frac{\|x_d^s - x_{d+1}^s\|^2}{2} + \frac{\theta_s^2 \|y_{t+1}^s - y_t^s\|^2}{2} \right] \\
&\leq \frac{L}{2} \sum_{d=D(t)}^{t-1} \mathbf{E} \|x_d^s - x_{d+1}^s\|^2 + \frac{L\theta_s^2\tau}{2} \mathbf{E} \|y_{t+1}^s - y_t^s\|^2.
\end{aligned} \tag{57}$$

Substituting (56) and (57) in (54), we get

$$\begin{aligned}
\mathbf{E}F(x_{t+1}^s) &\leq \mathbf{E} \left[(1 - \theta_s)F(\tilde{x}^{s-1}) + \theta_s F(x^*) + \frac{\theta_s}{2\eta_s} (\|x^* - y_t^s\|^2 - \|x^* - y_{t+1}^s\|^2) + \frac{\theta_s^3 \rho(b) LD}{2\tau} \right. \\
&\quad \left. + \underbrace{\frac{L}{2} \|x_{D(t)}^s - x_t^s\|^2 + \frac{L}{2} \|x_{t+1}^s - x_t^s\|^2 - \frac{\theta_s}{2\eta_s} \|y_{t+1}^s - y_t^s\|^2 + \frac{\tau L \theta_s}{2} \|y_{t+1}^s - y_t^s\|^2}_{T_5} \right] \\
&\quad + \underbrace{\frac{L}{2} \sum_{d=D(t)}^{t-1} \|x_d^s - x_{d+1}^s\|^2 + \frac{L\theta_s^2\tau}{2} \|y_{t+1}^s - y_t^s\|^2}_{T_6}.
\end{aligned} \tag{58}$$

On the other hand, since $\sum_{t=0}^{m-1} \sum_{d=D(t)}^{t-1} \|x_{d+1}^s - x_d^s\|^2 \leq \tau \sum_{t=0}^{m-1} \|x_{t+1}^s - x_t^s\|^2$, it can be verified that

$$\sum_{t=0}^{m-1} (T_5 + T_6) \leq \xi \sum_{t=0}^{m-1} \|y_{t+1}^s - y_t^s\|^2, \tag{59}$$

where $\xi = \left(\frac{L\tau^2\theta_s^2 + L\theta_s^2 + \tau L\theta_s + 2L\tau\theta_s^2}{2} - \frac{\theta_s}{2\eta_s} \right)$. Let $\eta_s \theta_s = \frac{1}{\sigma L}$ where $\sigma > 100$. It can be verified that if $\tau \leq \frac{\sqrt{(\frac{1}{\theta_s} + 2)^2 + 4(\sigma - 1) - (\frac{1}{\theta_s} + 2)}}{2}$, $\xi \leq 0$. Suppose the above constraint holds. Then, we have

$$\sum_{t=0}^{m-1} \mathbf{E}F(x_{t+1}^s) \leq \sum_{t=0}^{m-1} \mathbf{E} \left[(1 - \theta_s)F(\tilde{x}^{s-1}) + \theta_s F(x^*) + \frac{\theta_s}{2\eta_s} (\|x^* - y_t^s\|^2 - \|x^* - y_{t+1}^s\|^2) + \frac{\theta_s^3 \rho(b) LD}{2\tau} \right]. \tag{60}$$

Using $\tilde{x}^s = \frac{1}{m} \sum_{t=0}^{m-1} x_{t+1}^s$, we obtain

$$\mathbf{E} \left[F(\tilde{x}^s) - F(x^*) \right] \leq \mathbf{E} \left[(1 - \theta_s) (F(\tilde{x}^{s-1}) - F(x^*)) + \frac{\sigma L \theta_s^2}{2m} (\|y_0^s - x^*\|^2 - \|y_m^s - x^*\|^2) + \frac{\theta_s^3 \rho(b) LD}{2\tau} \right]. \tag{61}$$

Dividing both sides of (61) by θ_s^2 , summing over $s = 1$ to S , and using the definition $y_0^s = y_m^{s-1}$ and that $\frac{1 - \theta_s}{\theta_s^2} \leq \frac{1}{\theta_{s-1}^2}$ when $\theta_s = \frac{2}{s+2}$, we have

$$\mathbf{E} \left[F(\tilde{x}^S) - F(x^*) \right] \leq \frac{4 \left[F(\tilde{x}^0) - F(x^*) \right]}{(S+2)^2} + \frac{2\sigma L \|\tilde{x}^0 - x^*\|^2}{m(S+2)^2} + \frac{2\rho(b) LD \log S}{\tau(S+2)^2}. \tag{62}$$

□

13.3 Proof of Corollary 4

Proof of (a). When $s \leq n^{\frac{2}{3}}$, $b = s$, then $\rho(b) = \frac{n-b}{b(n-1)} \leq \frac{1}{b} = \frac{1}{s}$. In this case, T_3 in (56) can be bounded as (here we use T'_3 to indicate that it is a new bound)

$$\begin{aligned}
\mathbf{E}T'_3 &= \theta_s \mathbf{E} \langle \nabla f(x_t^s) - v_t^s, y_{t+1}^s - y_t^s \rangle \\
&\leq \frac{1}{2\tau L} \mathbf{E} \|\nabla f(x_t^s) - v_t^s\|^2 + \frac{\tau L \theta_s^2}{2} \mathbf{E} \|y_{t+1}^s - y_t^s\|^2 \\
&\leq \frac{\rho(b)}{2\tau L} \mathbf{E} \|\nabla f_{i_t^s}(x_t^s) - \nabla f_{i_t^s}(\tilde{x}^{s-1}) + \nabla f(\tilde{x}^{s-1}) - \nabla f(x_t^s)\|^2 + \frac{\tau L \theta_s^2}{2} \mathbf{E} \|y_{t+1}^s - y_t^s\|^2 \\
&\leq \frac{\rho(b)}{2\tau L} \mathbf{E} \|\nabla f_{i_t^s}(x_t^s) - \nabla f_{i_t^s}(\tilde{x}^{s-1})\|^2 + \frac{\tau L \theta_s^2}{2} \mathbf{E} \|y_{t+1}^s - y_t^s\|^2 \\
&\leq \frac{\rho(b)L^2}{2\tau L} \mathbf{E} \|x_t^s - \tilde{x}^{s-1}\|^2 + \frac{\tau L \theta_s^2}{2} \mathbf{E} \|y_{t+1}^s - y_t^s\|^2 \\
&= \frac{\theta_s^2 \rho(b) L^2}{2\tau L} \mathbf{E} \|y_t^s - \tilde{x}^{s-1}\|^2 + \frac{\tau L \theta_s^2}{2} \mathbf{E} \|y_{t+1}^s - y_t^s\|^2 \\
&\leq \frac{\theta_s^2 \rho(b) LD}{2\tau} + \frac{\tau L \theta_s^2}{2} \mathbf{E} \|y_{t+1}^s - y_t^s\|^2 \\
&\leq \frac{\theta_s^2 LD}{2\tau s} + \frac{\tau L \theta_s^2}{2} \mathbf{E} \|y_{t+1}^s - y_t^s\|^2.
\end{aligned} \tag{63}$$

Then, following the proofs from (57) to (62), we obtain (when $S \leq n^{\frac{2}{3}}$)

$$\mathbf{E} \left[F(\tilde{x}^S) - F(x^*) \right] \leq \frac{4 \left[F(\tilde{x}^0) - F(x^*) \right]}{(S+2)^2} + \frac{2\sigma L \|\tilde{x}^0 - x^*\|^2}{m(S+2)^2} + \frac{2LD \log S}{\tau(S+2)^2}, \tag{64}$$

as long as $\xi' = \left(\frac{L\tau^2\theta_s^2 + L\theta_s^2 + \tau L\theta_s^2 + 2L\tau\theta_s^2}{2} - \frac{\theta_s}{2\eta_s} \right) \leq 0$. Let $\eta_s = \frac{1}{\sigma L \theta_s}$, then τ needs to be smaller than $\frac{\sqrt{9+4(\sigma-1)}-3}{2}$.

□